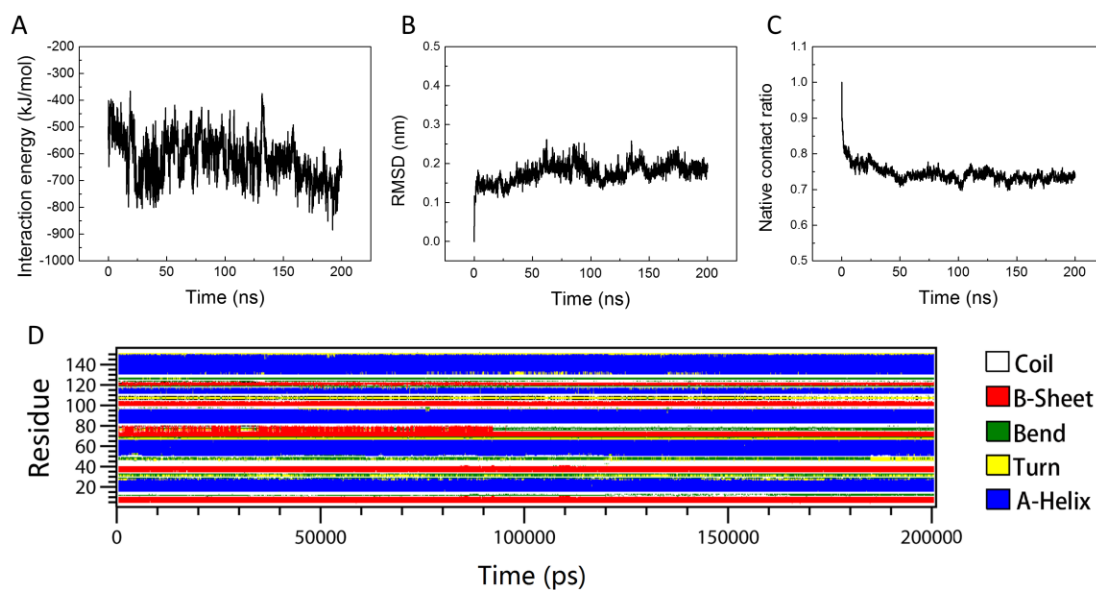


## **Revealing Cooperation between Knotted Conformation and Dimerization in Protein Stabilization by Molecular Dynamics Simulations**

Yan Xu,<sup>†,‡</sup> Shixin Li,<sup>†</sup> Zengshuai Yan,<sup>†</sup> Baosheng Ge,<sup>†</sup> Fang Huang,<sup>†</sup> and Tongtao Yue<sup>\*,†</sup>

<sup>†</sup>State Key Laboratory of Heavy Oil Processing, Center for Bioengineering and Biotechnology, College of Chemical Engineering, China University of Petroleum (East China), Qingdao 266580, China

<sup>‡</sup>College of Electronic Engineering and Automation, Shandong University of Science and Technology, Qingdao 266590, China



**Figure S1.** Stability of the knotted proteins in dimer. (A) Time evolution of the interaction energy at the dimer interface. (B) Time evolution of the RMSD for the knotted proteins in dimer. (C) Time evolution of the intramolecular native contact ratio for proteins. (D) Time evolution of the secondary structural change of one subunit in the dimer.

**Table S1.** All pairs of interactions between residues at the dimer interface. The first column lists all residues in the subunit B in contact with those in the subunit A (second column). The third column describes properties of the interactions. Background colors of green, blue and pink represent residues in the domains of respectively  $\alpha 1$ ,  $\alpha 3$  and  $\alpha 5$  in the subunit B.

Residues in subunit A	Residues in subunit B	Interaction property
15Trp	15Trp'	$\pi$ - $\pi$ stacking
15Trp	16Val', 19Gly', 20Phe', 134Val'	hydrophobic
16Val	15Trp'	hydrophobic
19Gly	15Trp'	hydrophobic
20Phe	15Trp'	hydrophobic
78Pro	124Ala'	hydrophobic
79Trp	124Ala', 125Leu'	hydrophobic
81Thr	126Thr'	H-bond
82Pro	125Leu'	hydrophobic
84Leu	125Leu'	hydrophobic
106Glu	142Arg', 153His'	electrostatic
120Trp	125Leu'	hydrophobic
122Leu	122Leu', 124Ala', 125Leu'	hydrophobic
124Ala	78Pro', 79Trp', 124Ala'	hydrophobic
125Leu	78Pro', 79Trp', 84Leu', 120Trp', 122Leu', 135Leu'	hydrophobic
126Thr	81Thr'	H-bond
127Leu	135Leu'	hydrophobic
128Pro	135Leu'	hydrophobic
129His	138Glu'	electrostatic
131Leu	131Leu', 134Val', 135Leu'	hydrophobic
134Val	15Trp', 131Leu'	hydrophobic
135Leu	127Leu', 128Pro', 131Leu', 135Leu'	hydrophobic
138Glu	129His'	electrostatic
142Arg	106Glu'	electrostatic

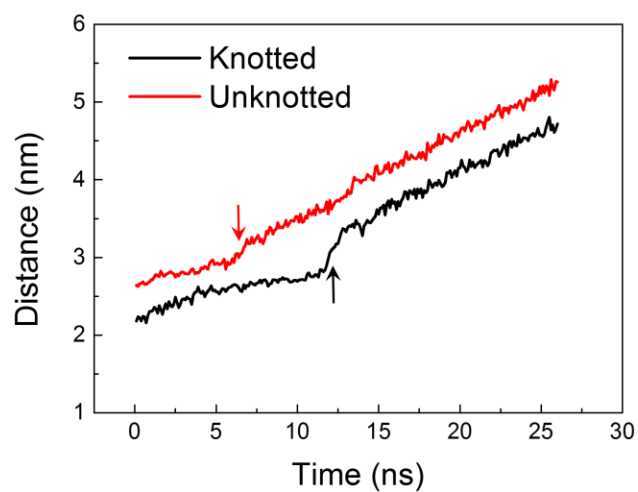


**Figure S2.** Time evolution of the distance between centers of two knotted proteins under an external force with the spring constant of  $1000 \text{ kJ/mol/nm}^2$ .

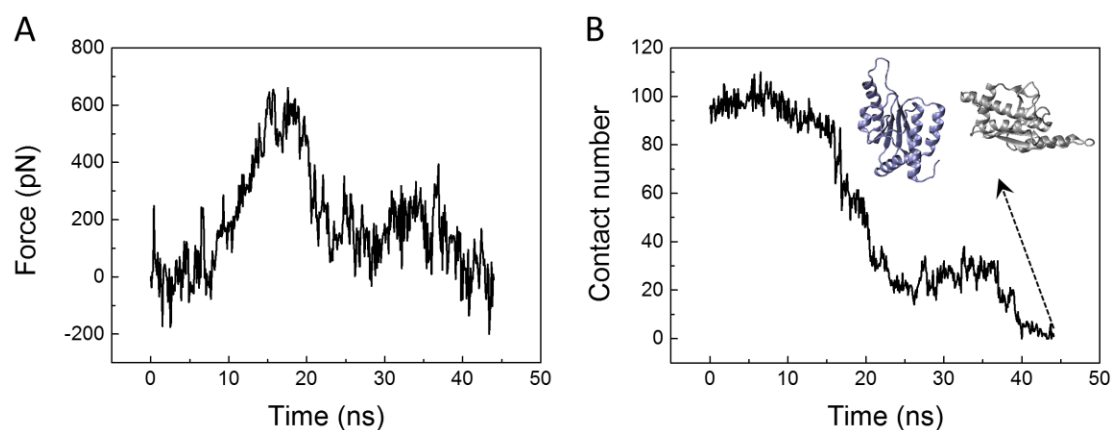


**Figure S3.** Mechanical response of the knotted proteins in dimer using a lower pulling velocity of 0.00005 nm/ps. (A) Time evolution of the pulling resistant force. (B) Time evolution of the number of contacts at the dimer interface. Inset of B shows the final simulated snapshot illustrating that two knotted proteins have been completely separated.

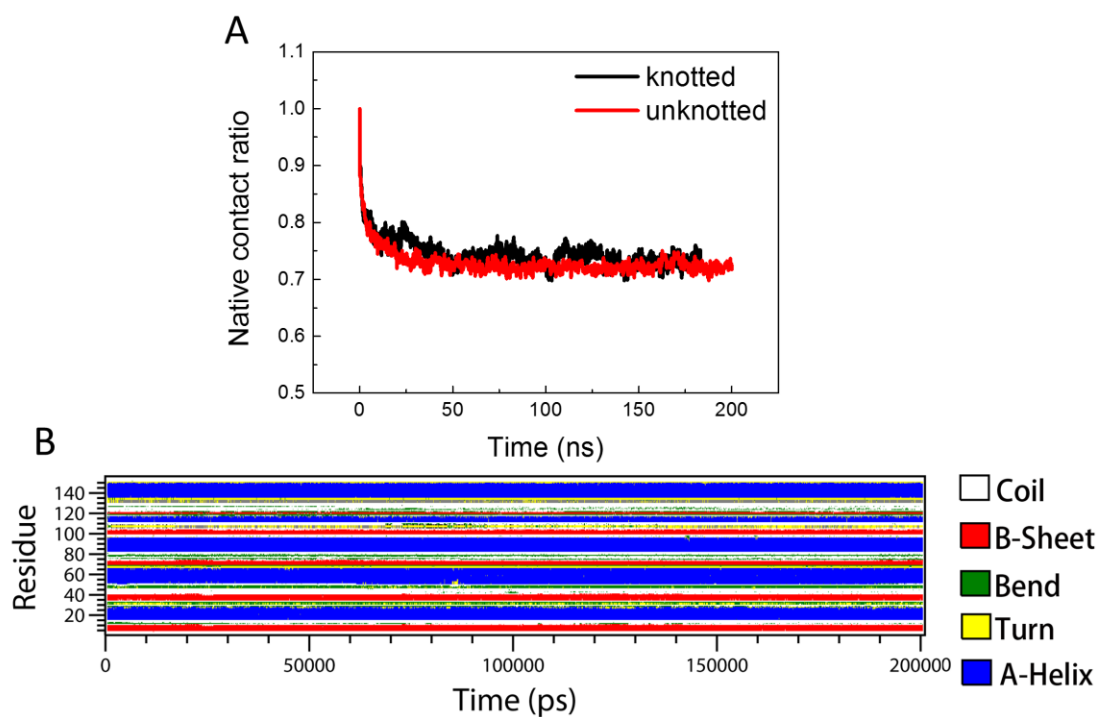


**Figure S4.** Stability of the unknotted proteins in dimer. (A) Time evolutions of the intramolecular native contact ratios for both the knotted and unknotted proteins in dimer. (B) Time evolution of the secondary structural change for the unknotted protein.

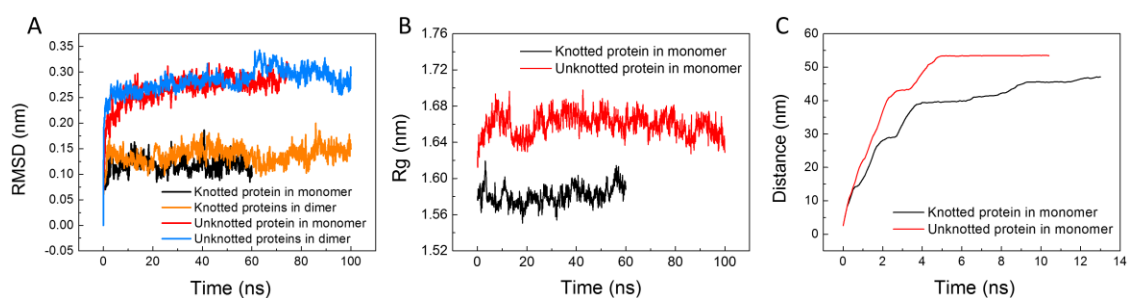


**Figure S5.** Knot stabilizing effect on proteins in monomer and dimer. (A) Time evolutions of the RMSD for proteins in four distinct systems, evidencing the stabilizing effect of knot on proteins in both monomer and dimer. (B) Time evolutions of the radius of gyration of knotted and unknotted proteins. (C) Time evolutions of the end-to-end distances for knotted and unknotted proteins in monomer under a constant mechanical stretching force of 400 kJ/mol/nm. Part of the mechanical stretching data was obtained from our previous simulation work.

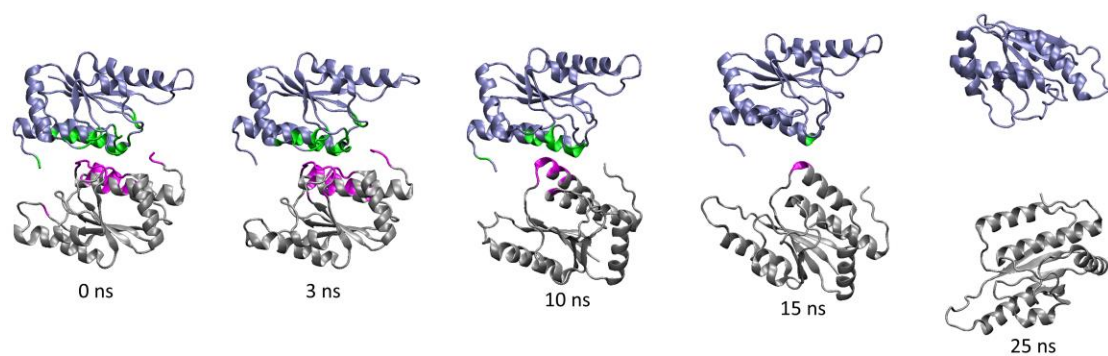


**Figure S6.** Time sequence of the typical snapshot depicting mechanical separation of dimeric proteins with the knot in each protein removed.

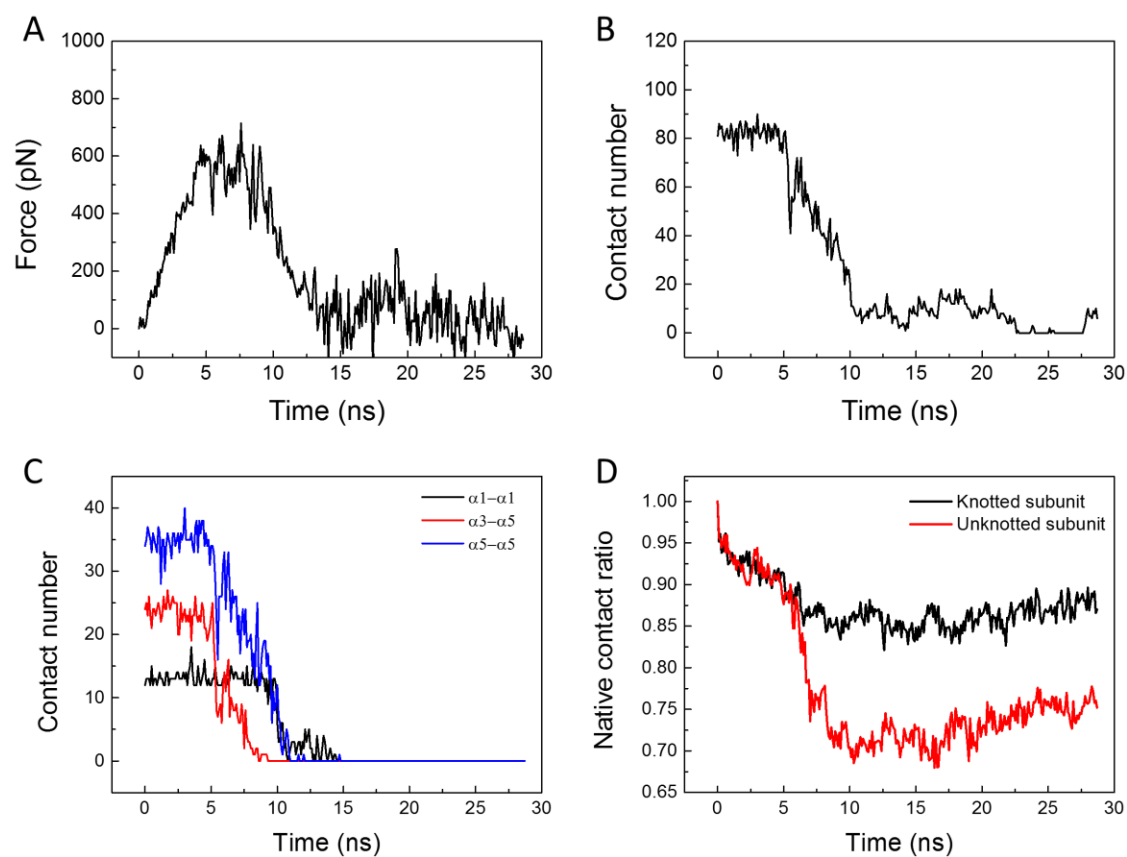


**Figure S7.** Mechanical separation of a heterodimer, in which the knot of one subunit is removed while the other is maintained. (A) Time evolution of the resistant force. (B) Time evolution of the interfacial contact number. (C) Time evolutions of the number of contacts between specific domains at the heterodimer interface. (D) Time evolutions of the native contact ratio for both the knotted and the unknotted subunits.

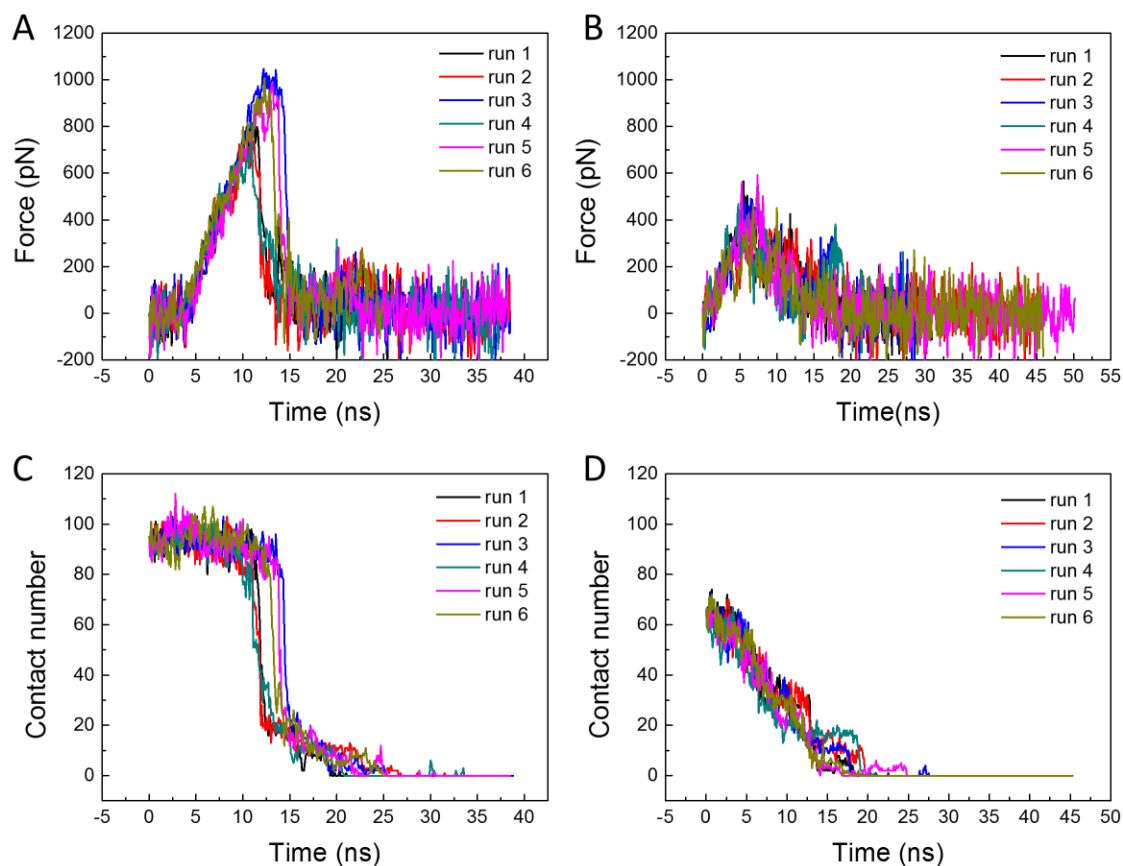


**Figure S8.** Six independent simulations of mechanical separation of two dimeric proteins with and without a knot in each subunit. (A) Time evolutions of the pulling resistant force for two knotted proteins in dimer. (B) Time evolutions of the pulling resistant force for two unknotted proteins. (C) Time evolutions of the number of contact at interfaces of two knotted proteins in dimer. (D) The number of contacts at interfaces of two unknotted proteins as a function of time.

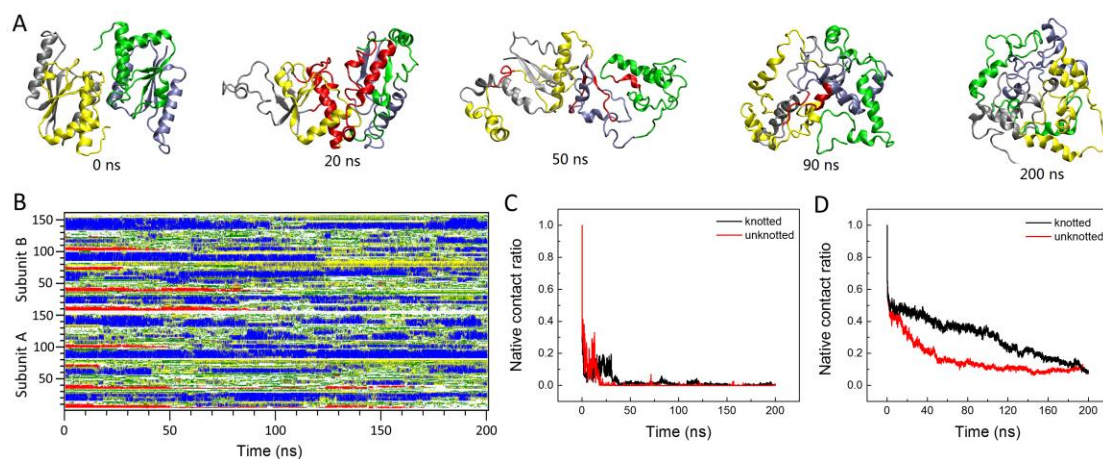


**Figure S9.** Thermal denaturation of unknotted proteins in dimer. (A) Time sequence of typical snapshots. The major secondary structural change at each step is highlighted by coloring in red. (B) Time evolution of the secondary structural change of each subunit in the dimer. (C) Time evolutions of the native contact ratio at the dimer interface of both knotted and unknotted proteins. (D) Time evolutions of the intramolecular native contact ratio for both knotted and unknotted proteins.